SUPPLEMENTARY MATERIAL

Mechanochemical Synthesis of Tungstophosphoric Acid Based High Efficiency Photocatalysts

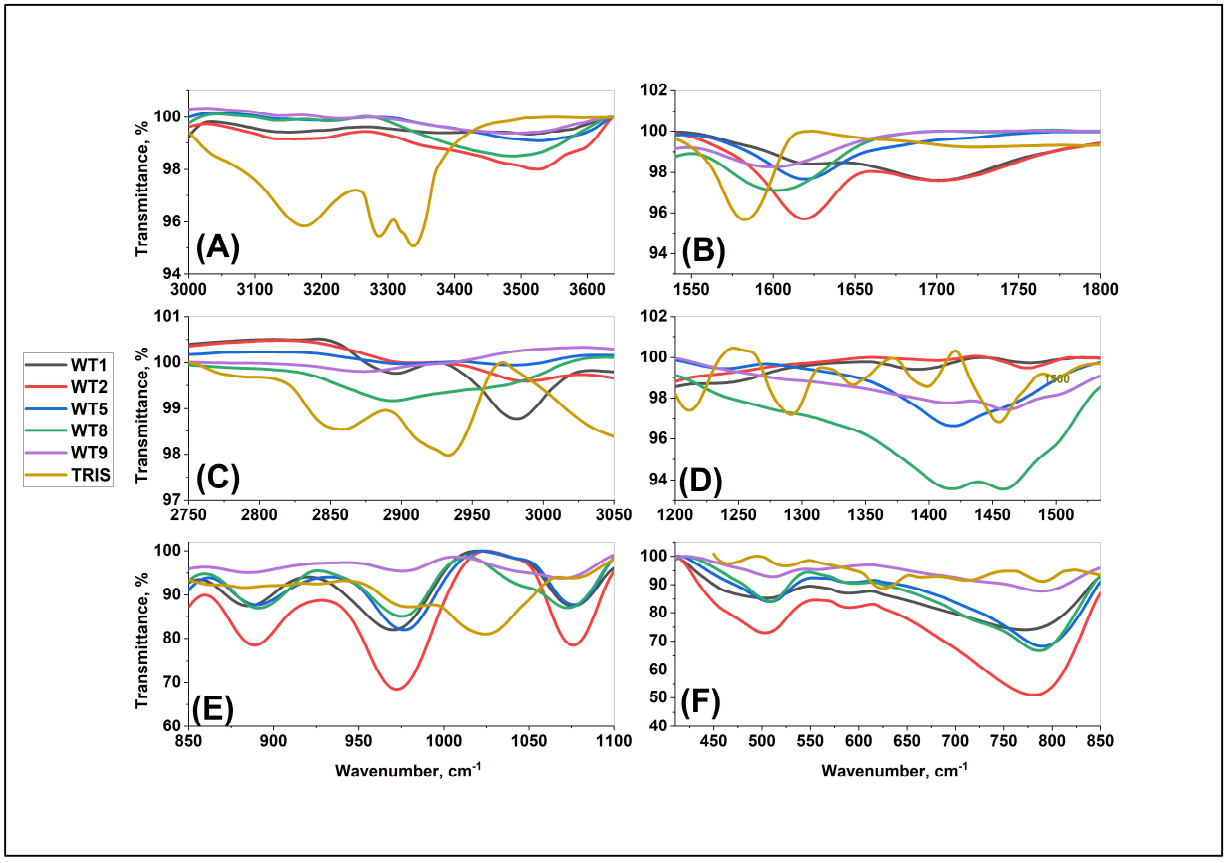

Figure S 1. Segmented ATR-IR spectra of TRIS and its hybrids with TPA (WT1 – WT9). Panels (A-D) highlight the organic-cationic environment and hydrogen bonding, whereas panels (E-F) display the fingerprint and skeletal vibrations of the inorganic polyoxometalate framework.

Table S 1. Infrared vibrational modes, their assignments and vibrational frequencies for pure tungstophosphoric acid (TPA), pure TRIS, and their hybrids (WT) as extracted from Figure S1 and reference [1].

Vibrational Mode & Assignment	**Infrared vibrational frequencies (cm^{-1})**						
	Pure TPA	**Pure TRIS**	**WT1**	**WT2**	**WT5**	**WT8**	**WT9**
ν(O−H) (TRIS/Hybrid)	—	3339	3513	3525	3528	3486	3482
ν(CH_2) Asymmetric	—	2933	2981	2987	2978	—	—
ν(CH_2) Symmetric	—	2858	2896	—	—	2894	2873
ν(N−H) Asymmetric	—	3287	3031-3274 (br)	3022-3272 (br)	3208	3211	3229
ν(N−H) Symmetric	—	3174			3133	3134	3142
δ(H_3O^+/$H_5O_2^+$) (Bend)	1701	—	1701	1701	—	—	—
δ(NH_2/NH_3^+) (Bend)	—	1583	1619	1619	1624	1602	1601
δ(CH_2) (Backbone)	—	1455	1480	1477	—	1461	1458
δ(OH) + ω(CH_2)	—	1398	1391	1406	1419	1419	1415
ν(C−N)	—	1211	1240	1240	—	—	—
ν(P−O_a) (Internal)	1075	—	1076	1076	1076	1073	1070
ν(W=O_t) (Terminal)	981	—	970	972	977	975	976
ν(W−O_c−W) (Corner)	886	—	885	889	890	891	885
ν(W−O_e−W) (Edge)	789	790 (NH_2 Wag)	771	781	790	786	789
Keggin Skeleton	590	—	590	591	592	596	—
Internal W−O_a−P	500	—	502	503	509	509	511

Table S 2. XRD Profile matching hybrid WT2 with standard TPA ((JCPDS 101-0874)

No.	Intensity [%]	d-spacing [Å]	2Theta [°]	HKL	Matched
1	100	8.587	10.293	0 1 1	TRUE
2	13.7	6.0704	14.58	0 0 2	TRUE
3	6.2	4.95584	17.884	1 1 2	TRUE
4	28.8	4.29238	20.676	0 2 2	TRUE
5	11	3.8397	23.146	0 1 3	TRUE
6	64.8	3.5046	25.394	2 2 2	TRUE
7	22.7	3.0352	29.404	0 0 4	TRUE
9	7.6	2.86183	31.229	1 1 4	TRUE
11	5.2	2.71483	32.967	0 2 4	TRUE
13	54.6	2.58831	34.628	2 3 3	TRUE
15	25.6	2.38105	37.751	0 1 5	TRUE
16	3.3	2.21675	40.668	1 2 5	TRUE
17	5.5	2.14619	42.067	0 4 4	TRUE
18	3.2	2.02347	44.752	0 0 6	TRUE
19	11.5	1.96947	46.048	2 3 5	TRUE
20	9.8	1.87331	48.56	1 4 5	TRUE
21	21.3	1.71704	53.31	0 5 5	TRUE
22	1.7	1.65211	55.582	3 3 6	TRUE
23	28.8	1.54188	59.945	2 3 7	TRUE
24	10.2	1.49448	62.052	4 5 5	TRUE

Table S 3. XRD Profile matching hybrid WT5 with standard TPA (JCPDS 101-0874)

No.	Intensity [%]	d-spacing [Å]	2Theta [°]	HKL	Matched
1	100	8.587	10.293	0 1 1	TRUE
2	6.2	4.95584	17.884	1 1 2	TRUE
3	28.8	4.29238	20.676	0 2 2	TRUE
4	11	3.8397	23.146	0 1 3	TRUE
5	64.8	3.5046	25.394	2 2 2	TRUE
6	22.7	3.0352	29.404	0 0 4	TRUE
7	54.6	2.58831	34.628	2 3 3	TRUE
8	25.6	2.38105	37.751	0 1 5	TRUE
9	11.5	1.96947	46.048	2 3 5	TRUE
10	9.8	1.87331	48.56	1 4 5	TRUE
11	21.3	1.71704	53.31	0 5 5	TRUE
12	28.8	1.54188	59.945	2 3 7	TRUE
13	0	1.5176	61.005	0 0 8	TRUE
14	10.2	1.49448	62.052	4 5 5	TRUE

Table S 4. Rietveld refinement results for hybrids WT2 and WT5. The values in parenthesis for crystallite size were obtained from Williamson-Hall plots of the hybrids.

Structural Category	Parameter	TPA (96-101-0874)	WT2	WT5
Refinement Quality	Weighted Profile R-factor (R_{wp}) %	—	22.72	18.06
	Goodness of Fit (χ^2)	—	3.62	1.98
Unit Cell (Cubic)	Lattice Constant (a) Å	12.1410	12.217	12.206
	Unit Cell Volume (V) Å^3	1789.63	1823.52	1818.60
Microstructure	Crystallite Size (D) nm	—	52.7 (59.9)	51.5 (53.9)
	Micro-strain (ϵ) x 10^{-3}	—	4.21	4.47
Internal Geometry	Avg. $W-O$ Bond Length Å	—	2.172	2.169
	Octahedral Distortion Index (D)	Symmetric	0.2178	0.2183

Table S 5. Extent of lattice expansion observed for WT2 and WT5 induced by TRIS incorporation.

Material	Lattice Constant (a) Å	(Δa) Å	Total Volume (V) Å^3	Volumetric Expansion %
Parent TPA	12.1410	—	1789.63	—
WT2 (4:1)	12.2170	+0.076	1823.52	1.89
WT5 (1:1)	12.2060	+0.065	1818.60	1.62

Table S 6. Mathematical relationships used to determine kinetic and other parameters to highlight dye removal efficiency of hybrids

Parameter	Units	Equation	Description of Variables
Degradation Efficiency	%	$\eta = \frac{C_0 - C_t}{C_0} \times 100$	C_0: Initial dye concentration; C_t Concentration at time t.
Apparent Rate Constant (k_{app})	min^{-1}	$ln\left(\frac{C_0}{C_t}\right) = k_{app}t$	t: Irradiation time in minutes; k_{app}: Slope of the linear regression.
Adsorption Constant (K_{ads})	mM^{-1}	$\frac{1}{k_{app}} = \frac{1}{kK_{ads}} + \frac{C_0}{k}$	k: Specific rate constant (mM · min^{-1}); K_{ads}: Surface affinity coefficient.
Specific Degradation Rate (SDR)	$\text{mmol} \cdot \text{g}^{-1} \cdot \text{h}^{-1}$	$\text{SDR} = \frac{(C_0 - C_t) \times V}{m \times t}$	V: Solution volume (L); m Catalyst mass (g); t: Time (h).
Synergy Index (S.I.)	Dimensionless	$\text{S.I.} = \frac{k_{app(hybrid)}}{k_{app(TPA)}}$	$k_{app(hybrid)}$: Rate of WT series; $k_{app(TPA)}$: Rate of Pure TPA.

Table S 7. Percent dye removal by TPA and hybrids and its correlation with catalyst dose and dye concentration.

Dye Conc.	Catalyst	MG Removal by Different Quantities of Catalysts				
		0.4 g	**0.8 g**	**1.2 g**	**1.6 g**	**2.0 g**
0.1 mM	Pure TPA	62.15%	70.40%	78.71%	81.20%	76.45%
	WT1	93.12%	95.18%	96.41%	—	—
	WT2	45.20%	55.10%	61.79%	—	—
	WT5	88.15%	92.40%	95.12%	—	—
	WT8	33.07%	95.38%	97.69%	—	—
	WT9	92.10%	96.50%	98.46%	—	—
0.5 mM	Pure TPA	85.30%	91.15%	95.13%	96.10%	92.20%
	WT1	—	—	95.29%	—	—
	WT2	—	—	96.97%	—	—
	WT5	—	—	94.12%	—	—
	WT8	—	—	93.78%	97.47%	93.61%
	WT9	—	—	95.96%	—	—
1.0 mM	Pure TPA	80.20%	86.50%	92.67%	94.15%	90.30%
	WT1	94.15%	96.22%	97.61%	—	—
	WT2	82.40%	88.15%	92.53%	—	—
	WT5	91.30%	94.50%	97.04%	—	—
	WT8	89.43%	94.22%	97.05%	—	—
	WT9	88.50%	92.10%	94.50%	—	—

Table S 8. Kinetic parameters for malachite green (MG) removal by TPA and hybrids and their correlation with catalyst dose and dye concentration.

Conc.	Catalyst	Dosage	k_{app} (min^{-1})	K_{ads} (mM^{-1})	S.I.	SDR ($mmol \cdot g^{-1} \cdot h^{-1}$)
0.1 mM	Pure TPA	0.4 g	0.0152	0.003	1.0	0.155
		0.8 g	0.0195	0.003	1.0	0.088
		1.2 g	0.0258	0.004	1.0	0.065
		1.6 g	0.0281	0.004	1.0	0.051
		2.0 g	0.0243	0.004	1.0	0.038
	WT1	1.2 g	0.0554	0.015	2.15	0.08
	WT2	1.2 g	0.016	0.009	0.62	0.051
	WT5	1.2 g	0.0503	0.042	1.95	0.079
	WT8	0.4 g	0.0067	0.051	0.44	0.083
		0.8 g	0.0513	0.053	2.63	0.119
		1.2 g	0.0628	0.055	2.43	0.081
	WT9	1.2 g	0.0696	0.061	2.7	0.082
0.5 mM	Pure TPA	1.2 g	0.0504	0.006	1.0	0.396
		1.6 g	0.0521	0.006	1.0	0.301
		2.0 g	0.0443	0.006	1.0	0.231
	WT1	1.2 g	0.0509	0.018	1.01	0.397
	WT2	1.2 g	0.0583	0.012	1.16	0.404
	WT5	1.2 g	0.0474	0.048	0.94	0.392
	WT8	1.2 g	0.0456	0.057	0.9	0.39
		1.6 g	0.0612	0.059	1.17	0.304
		2.0 g	0.0458	0.059	1.03	0.234
	WT9	1.2 g	0.0535	0.063	1.06	0.399
1.0 mM	Pure TPA	0.4 g	0.0264	0.008	1.0	2.005
		0.8 g	0.0341	0.008	1.0	1.081
		1.2 g	0.0435	0.008	1.0	0.772
		1.6 g	0.0461	0.009	1.0	0.588
		2.0 g	0.0402	0.009	1.0	0.452
	WT1	1.2 g	0.0622	0.021	1.43	0.813
	WT2	1.2 g	0.0431	0.014	0.99	0.771
	WT5	1.2 g	0.0586	0.052	1.35	0.808
	WT8	0.4 g	0.0374	0.059	1.42	2.236
		0.8 g	0.0475	0.061	1.39	1.178
		1.2 g	0.0587	0.064	1.35	0.808
	WT9	1.2 g	0.0483	0.07	1.11	0.787

1. ALHARTHI AI. Efficient Catalytic Performance of Calcined Tungstophosphoric Acid for the Claisen-Schmidt Condensation under Solvent-Free Reaction. Asian J Chem. 2019;31(11):2579–84.